European Journal of Applied Sciences – Vol. 13, No. 04
Publication Date: July 23, 2025
DOI:10.14738/aivp.1304.19134.
Quinn, H. M. (2025). A Comparison of Sir Osborne Reynold's 1883 Seminal Paper and the QFFM: A Hand in Glove Reconciliation. *European Journal of Applied Sciences*, Vol - 13(04). 71-92.

A Comparison of Sir Osborne Reynold's 1883 Seminal Paper and the QFFM: A Hand in Glove Reconciliation

Hubert M Quinn
The Wrangler Group LLC., 40 Nottinghill Road, Brighton, Ma. 02135

ABSTRACT

Since Sir Osborne Reynolds wrote his seminal paper in 1883 in which he unveiled, for the first time, the elements of what would become the governing equation for fluid flow in closed conduits and which bears his name to this day, much confusion has surrounded the explanation for the phenomenon typically referred to as the fluid flow regime. In a follow up development circa 1904, Ludwig Prandtl and his students developed a concept known today as the viscous boundary layer which has to do with fluid flow adjacent to a solid boundary. Many consider this concept as a vital underpinning for modern day aerodynamics. In addition to these two fundamental developments, Johann Nikuradze who, incidentally, was one of Prandtl's students, circa 1933 published his critical experiments in which he glued sand particles to the inner walls of conduits forming what stands as the gold standard, even to this day, for permeability measurements in roughened pipes. In the parallel field of study involving packed beds, John Calvin Giddings in 1965 outlined a teaching of permeability unprecedented in the published literature for conduits packed with solid obstacles. This appeared in the first of his two classic text books on this subject matter. These teachings and concepts for both packed and empty conduits have dominated the conversation of fluid flow in closed conduits for the best part of the last 150 years but without any coherent explanation of how they all combine, within the dictates of the Laws of Nature, to produce the complicated flow patterns we currently associate with the change in flow profile, from laminar to turbulent flow. The advent of the Quinn Fluid Flow Model (QFFM), however, first published in 2019, provides the missing understanding of how these concepts come together. In this paper, we will demonstrate how this is accomplished by using the original publications of these fluid dynamic icons to validate the teaching of the QFFM, over 13 orders of magnitude of the Reynolds number. Additionally, we will show that fluid flow in an empty conduit is merely a special case of fluid flow in a conduit packed with solid obstacles. Moreover, we will demonstrate that turbulent flow is a highly structured form of fluid motion, driven by forces easily quantified within the context of the QFFM and is represented, within the Hypothetical Q Channel (HQC), as a form of damped simple harmonic motion, wherein the two damping mechanisms are, (1) wall friction, and (2) fluid internal friction. Finally, we will demonstrate that Reynold's observations regarding the transition from laminar to turbulent flow, in which he noticed a straight line of dye in the middle of the tube representing laminar flow, followed by a succession of eddies, representing the transition to turbulent flow, are replicated, virtually identically, in the QFFM teaching of damped curvy-linear simple harmonic motion in the HQC.

Keywords: Damped Harmonic Motion, Uniform Circular Motion, Turbulent Flow Tipping Point, Hypothetical Q Channel, Packed Conduit Porosity Function, Viscous Contributions, Kinetic Contributions, Reynolds Number.

INTRODUCTION

Beginning with the work of Darcy in packed conduits circa 1856 [1] and continuing to this very day, extraordinary amounts of energy has been expended by authors of scientific publications in an attempt to shed light on an understanding of underlying contributions to permeability, not only in packed conduits, but also in empty conduits.

Azevedo et al focused their attention on turbulent flow of water in corrugated pipes [2]. Baker et al studied the flow of air through packed conduits containing spherical particles [3]. Erdim et al studied the pressure drop-flow rate correlation of spherical powdered metal particles in packed conduits [4]. Dukhan et al, studied pressure drop in porous media with an eye to reconciliation with classical empirical equations [5]. Anspach et al reported results relating to very high pressure drops in very narrow id HPLC columns using small fully porous particles [6]. Zhong et al. studied air flow through sintered metal particles in the context of the Ergun flow model [7]. Tian et al reported experimental results with sintered ore particles in packed conduits [8]. Mayerhofer et al studied the permeability of irregularly shaped wood particles [9]. Pesic et al studied the effect of temperature on permeability of packed conduits containing spherical particles [10]. Abidzaid et al discusses water flow through packed beds in light of some modified equations [11]. Mirmanto et al studied friction factor of water in micro channels [12]. Capinlioglu et al focused his work on simplified correlations of packed bed pressure drops [13]. Yang et al made comparisons of superficially porous particles in packed HPLC columns [14]. Lundstrom et al used sophisticated analysis techniques to evaluate transitional and turbulent flow in packed beds [15]. Sletfjerding et al reported flow experiments with high pressure natural gas in empty pipes [16]. Langeiandsvik et al studied pipeline permeability and capacity [17]. De Stephano et al studied the performance characteristics of small particles in packed conduits for fast HPLC analysis [18]. Pereira reported on expected pressure drops in commercial HPLC columns [19]. Van Lopik et al studied grain size on nonlinear flow behavior [20]. Li et al discussed particle diameter effects in sand columns [21].

Carman modified the Kozeny/ Blake equation for laminar flow in packed conduits by including a term to accommodate irregularly shaped particles [22, 23, 35]. Coulson published his PhD thesis on laminar flow through packed conduits containing spherical particles [25]. Guiochon published his text book on packed conduits for use in preparative liquid chromatography [26]. Quinn published on laminar flow in packed conduits [27, 28, 29]. Ergun published on particles of coke packed in conduits in support of his now famous Ergun equation [30, 31]. The classic chemical engineering textbook by Lightfoot et al dealt with packed conduits in both laminar and transitional flow regimes [32]. J.C. Giddings published two classic textbooks on separation science both dedicated to the use of particles in packed conduits to achieve separations of small molecules [33, 34]. The original publication by Quinn on both packed and empty conduits appeared in 2019 [24]. Forchheimer published on packed conduits in which kinetic contributions were significant [36]. Farkas et al made measurements of permeability in the laminar flow regime in an effort to validate Darcy's law [37]. Kang published his master of science thesis on pebble bed reactors [38]. Buckwald et al published on roughened particles in packed conduits [39]. Nikuradze published his two classic studies of smooth and roughened pipes [40, 41]. Prandtl et al studied the effect of viscosity on flow near a solid boundary [42]. McKeon et al published the results of experiments in the now famous superpipe flow loop at

very high values of the Reynolds number [42, 43]. Studies at Oregon university used various gases at very high Reynolds number in open pipes [44].

THE QUINN FLUID FLOW MODEL (QFFM)

We begin by referring to the original publication of the QFFM [24]. Since much of the theoretical development of this comprehensive topic is outside the scope of this paper, we recommend that the reader look to that original document for proofs and details as needed.

The HQC

The Q-Porosity Function (ε):

Let us now collect all the partial porosity definitions in the QFFM underlying packed conduits which are defined in terms of particle size equivalents and view them as dimensionless mathematical functions of n_p, which we will designate as Q-Porosity functions. There is a total of 5 such functions, which we view in the context of the generalized Q-Porosity function ε.

1. $p_f = (1-\varepsilon_0) = n_p/n_{pq}$, the packed conduit particle volume fraction (p_f)
2. $\varepsilon_{sk} = (1-\varepsilon_p)\, n_p/n_{pq}$, the packed conduit solid skeletal volume fraction
3. $\varepsilon_0 = (1-n_p/n_{pq})$, the packed conduit external volume fraction
4. $\varepsilon_i = \varepsilon_p(n_p/n_{pq})$, the packed conduit internal volume fraction
5. $\varepsilon_t = 1-(1-\varepsilon_p)\, n_p/n_{pq}$, the packed conduit total volume fraction

Where n_p = number of particles of diameter d_p in any packed conduit under study, n_{pq} = the volume of the empty conduit under study expressed in number of particle equivalents of diameter d_p, d_p = average spherical particle diameter equivalent and ε_p = particle porosity.

Solid Nonporous Particles ($\varepsilon_p = 0$):

For the purposes of this discussion, we will only consider non-porous solid particles which eliminates #2 and #4 and leaves just three porosity categories, #1, #3 and #5. In Fig.1 we show a plot of these three porosity functions.

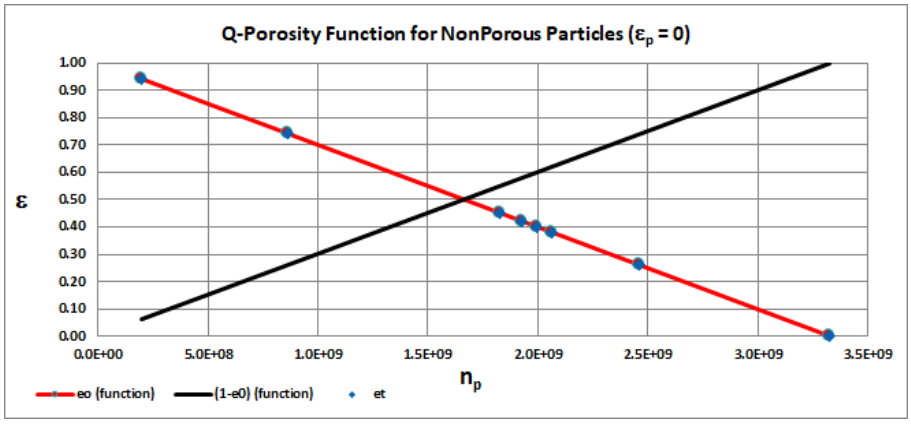

Fig. 1

As shown in Fig. 1, we see that for nonporous solid particles, the packed conduit external porosity ε_0 is identical to the packed conduit total porosity ε_t and, most importantly, both categories are always less than unity. This is because of the dictates of the Laws of Nature that

solid matter and free space are mutually exclusive and the reality of Kepler's conjecture which states that the maximum solid particle fraction one can achieve is about 0.74%, meaning a maximum value for the packed conduit particle fraction $p_f = (1-\varepsilon_0) = 0.74$ and the corresponding minimum value of $\varepsilon_0 = 0.26$.

Hypothetical Q-Particles ($\varepsilon_p = 1$):

We shall now consider the *special case* when the particles are *fully* porous, i.e., they are completely made of free space ($\varepsilon_p = 1$), i.e., a conduit devoid of obstacles. This scenario is presented in Figure 2.

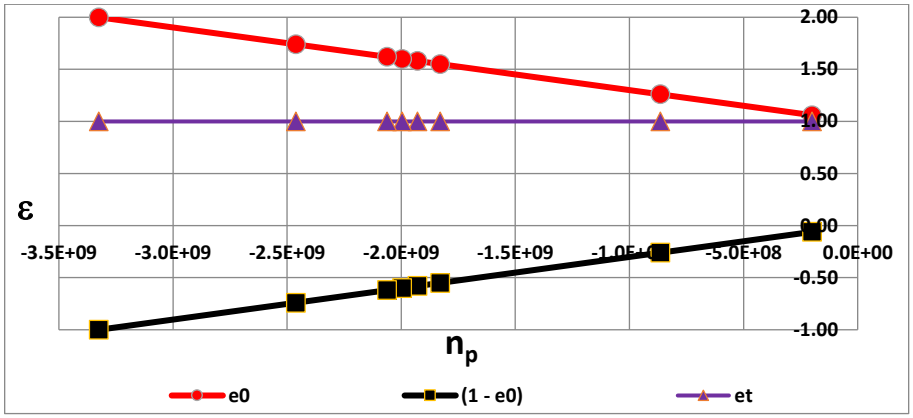

Fig. 2

As shown in Figure 2, our conduit packing process for particles made of free space ($\varepsilon_p = 1$), which we designate as hypothetical Q-particles, is represented by increasingly *negative* values of $\mathbf{n_p}$. Accordingly, the domain of the Q-Porosity function runs from 0 to - n_{pq}. Similarly, it follows that the range of the function varies between the values of -1 and 2, as shown in the plot. Note, in particular, that this plot appears to suggest an apparent contradiction, i.e., that the value of the packed conduit external porosity ε_0 is greater than unity. This is not a contradiction, however. Note that, in this case, the value of ε_t is always unity ($\varepsilon_t = 1.0$) for all values of n_p and, therefore, the Laws of Continuity are maintained. Note also that when the value of $n_p = -n_{pq}$, i.e., an empty conduit filled with particles of free space, the value of $\varepsilon_0 = 2.0$ and the value of the packed conduit particle fraction $p_f = -1.0$. The sum of the two porosities $\varepsilon_t = (\varepsilon_0 + p_f) = 1.0$. This is a valid representation because, in this scenario, there is no solid matter within the packed conduit and both the particle fraction p_f and the external porosity fraction ε_0 is comprised of free space which is all-inclusive and can, therefore, intermingle/overlap. Thus, from the point of view of the Laws of Nature, continuity is maintained because $\varepsilon_t = 1$ is consistent with all the free space within the packed conduit being available for fluid access, on the one hand, and, on the other hand, because the particle fraction $p_f = -1.0$ overlaps the external porosity fraction $\varepsilon_0 = 2.0$, providing a net total porosity $\varepsilon_t = 1$, the integrity of the mathematical model of the QFFM is maintained identical for packed conduits containing either solid particles or particles made of free space.

The Hypothetical Q Channel (HQC) Defined

Let us define a hypothetical *cylindrical* fluid channel representing a packed conduit, which we shall call the hypothetical Q channel (HQC), whose characteristic dimension is defined as $d_c = d_p / (\text{abs}(p_f)$. We can show this as a graphical representation in Fig. 3.

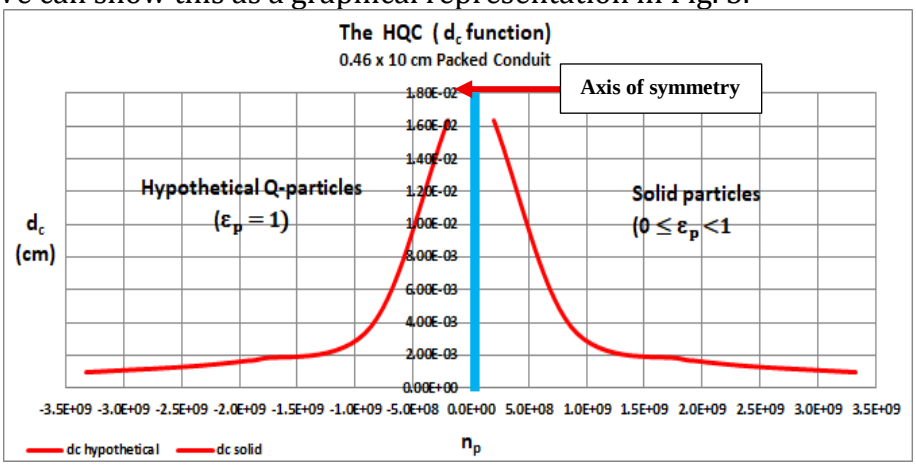

Fig. 3

As shown in Fig. 3, the HQC forms a mirror image on both sides of the axis of symmetry which is the dividing line represented by the line for $n_p = 0$.

We can now verify that the HQC representing both hypothetical and solid particles is identical by changing the x-axis from ($-n_p$) to abs (n_p) as shown in Fig. 4

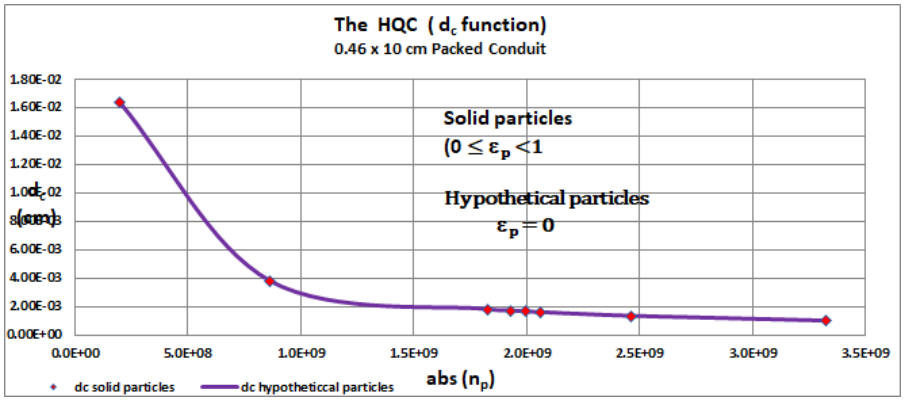

Fig. 4

Note that in Fig.4, the line representing the HQC for both type of particles collapses onto the same line.

The Critical Reynolds Number Value ($Re_{m\text{-}C}$ = 2,222) for Transition to Turbulent Flow

The pressure driven flow of fluids through closed conduits has never been fully understood. In fact, the Navier-Stokes equation which is generally recognized as the mathematical basis for describing the phenomenon, stands without analytical solution, even to this very day. Indeed, the Mathematical Institute of Cambridge, UK. offers one million dollars as an award for whomever provides the correct mathematically driven solution for this remaining puzzle of fluid dynamics. There is a recognizable *bona fides* for the fluid flow profile, however, which was

established in 1883 by none other than Sir Osborne Reynolds himself. Especially important to non-mathematically driven practitioners, this *bona fides* can be used instead of an advanced mathematically driven solution to the Navier-Stokes equation. In this now famous experiment by Reynolds, which was captured in black-and-white images, the apparatus and methodology of which is embarrassingly simple, the critical transition from laminar flow to turbulent flow can easily be observed with the naked eye, based upon the action of a colored dye in a flowing stream of water in an empty see-through conduit. The experiment, which is easily visible nowadays in a video on YouTube, clearly demonstrates that between the values for the now well-documented Reynolds number, R_e, of 2,100 and 2,300, there is a dramatic change in the fluid flow profile. Below a Reynolds number value of 2,100, the colored dye forms a straight line down the middle of the circular conduit. This fluid flow profile represents that of laminar flow in which there is no motion of the fluid in the radial direction. Above a value of the Reynolds number of 2,300, however, the fluid motion takes on a radial component, easily visible as clusters of eddies in the dye impregnated fluid. This fluid flow profile represents the condition now commonly referred to as the onset of turbulent flow. This was the crucial experiment in 1883 that enabled Reynolds to define the formula which now bears his name and hence his ability to document the range of values within which this transition occurs in the fluid flow regime. Although Reynolds did not offer any rational mechanistic basis for this change in fluid flow profile, the QFFM doctrine captures accurately, not only, the observations made by Reynolds, but also, a detailed mathematical model capable of replicating his experimental findings, as can be seen in Fig. 5 below.

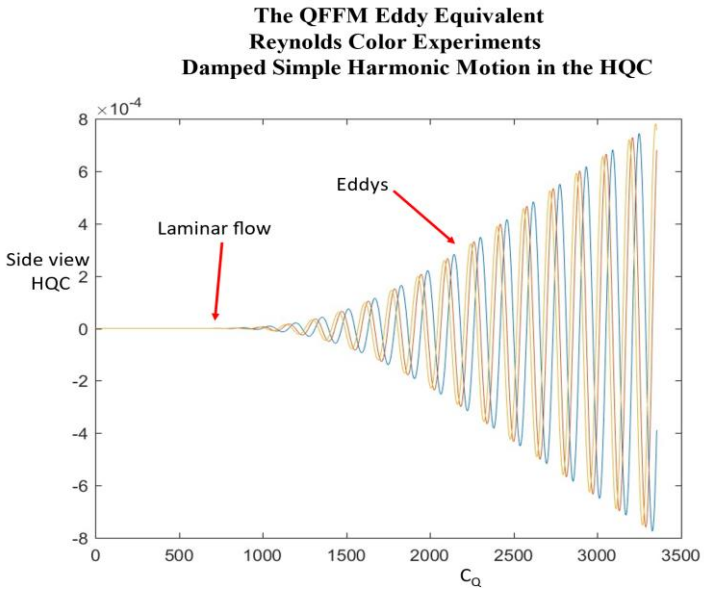

Fig. 5

As shown in Fig. 5, the fluid motion within the HQC is represented as a form of uniform circular motion which translates to curvy-linear damped simple harmonic motion. It is clear that this model easily captures and replicates the observations made by Reynolds in 1883.

Although there is consensus in the scientific community regarding the range of R_e number values of 2100 to 2300, within which the transition happens, there is no consensus on what

precisely causes the transition and where exactly in this range the critical value of the Re number occurs, up until now. With the advent of the QFFM in 2019, the mysterious tipping point in this range of values of the Re number is now apparent. This significant breakthrough in understanding has only come about as a result of the theoretical underpinnings of this new model, wherein fluid flow in closed conduits is defined in terms of it being a packed conduit of particles. In other words, the model dictates a duality of characteristics for pressure driven fluid flow in closed conduits which can be viewed as a Hypothetical Q Channel formed by conduits packed with particles, having either a solid skeleton or made of free space, the one being the mirror image of the other. This is the first theoretical model that defines fluid flow in an empty channel to be equated to flow in a packed conduit. Conventional wisdom always took the opposite view, i.e., fluid flow in a packed conduit to be equated to flow in an empty channel. The former concept, however, turns out to be a far superior methodology because there are many more measurable parameters to define the physics underlying the flow embodiment, resulting in a much better understanding of the interplay of the physical components responsible for the pressure/flow relationship. As a result of this fundamental difference in thinking, the physics underlying pressure driven fluid flow can now be validated in precise mathematical terms which leads directly to the determination of the precise tipping point, i.e., a critical Reynolds number value, $R_{em\text{-}C} = 2{,}222$ wherein the fluid flow profile undergoes transition from laminar to turbulent flow.

The QFFM is derived based upon the teaching of Forchheimer which dictates that the hydraulic pressure gradient, $[i = \Delta P/(\rho_f g L) = (a\mu_s + b\mu_s^2)$, as the driving mechanism behind flow in closed conduits, is a quadratic function of the fluid flux, i.e., fluid average superficial velocity (μ_s). The linear and quadratic coefficients of this second order polynomial mathematical expression, a and b, respectively, known as the Forchheimer coefficients, are utilized in the QFFM as the basis to define the precise makeup of the two fundamental contributing mechanisms to the physics of a packed bed of particles, underlying the fluid flow. These two contributing mechanisms, one linear with respect to fluid velocity which we call the viscous contribution, and one quadratic with respect to fluid velocity which we call the kinetic contribution, are the basis upon which the tipping point in the fluid flow profile is identified. We define this critical Reynolds number value, $R_{em\text{-}C} = 2{,}222$ as that precise point in the fluid flow regime of an empty conduit when the relative contributions of viscous and kinetic sources are identical. We can represent this Turbulence Tipping Point (TTP) graphically as the intersection of two lines on a plot, the x-axis of which is logarithmic to the base 10, i.e., log (2222) = 3.35, as shown below:

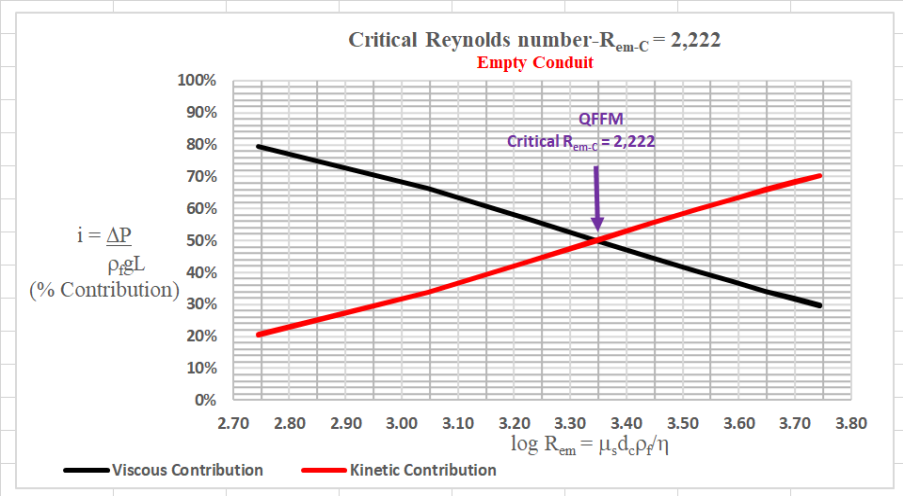

Fig. 6

As shown in Fig. 6, at the lowest values of the R_{em} shown, the viscous contribution ($a\mu_s$) represents 80% and the kinetic contribution ($b\mu_s^2$) represents 20% of the total hydraulic gradient. As the value of the modified Reynolds number R_{em} increases, the relative kinetic contribution increases, whereas the relative viscous contribution decreases. Ultimately, we reach the tipping point at 50% for each contribution which occurs, in the case of an empty conduit, at a value for log (2222) = 3.35. Below the R_{em} value of 2,222 the fluid flow profile is laminar flow; above the R_{em} value of 2,222 the fluid flow profile is in transition to turbulent flow.

Benchmarking Conventional Wisdom:

Now that we have a precise model to evaluate the fluid flow profile, we can use it to benchmark the accepted folklore in conventional wisdom relative to accepted marker values. An important marker in conventional wisdom relating to fluid flow through packed beds of solid particles, the Kozeny/Carman constant, K_c, is one such value that has caused much controversy throughout the last century approximately. Since this value is embedded in the Ergun fluid flow model, we can use the Ergun model to benchmark two values for Kc which have been foremost amongst the many erroneous values used in the published literature. To accomplish this task, we can simply use the QFFM model to test whether the Ergun constant A, also known as the Kozeny/Carman constant K_c, passes muster relative to the *bona fides* value of Reynolds for transition to turbulence, i.e., the range of values for Re of 2100-2300. We can show this analysis on a similar plot as above.

As shown in Fig, 7, the Ergun model which contains a value for K_c = 150 when evaluated in light of the QFFM, identifies the TTP to be at a value of the R_e of 86 for an empty conduit. This value is far too low as compared to the Reynolds *bona fides* range of 2100 to 2300. Additionally, using a value for K_c = 180 does not fare much better when compared to this new benchmark of 2,222.

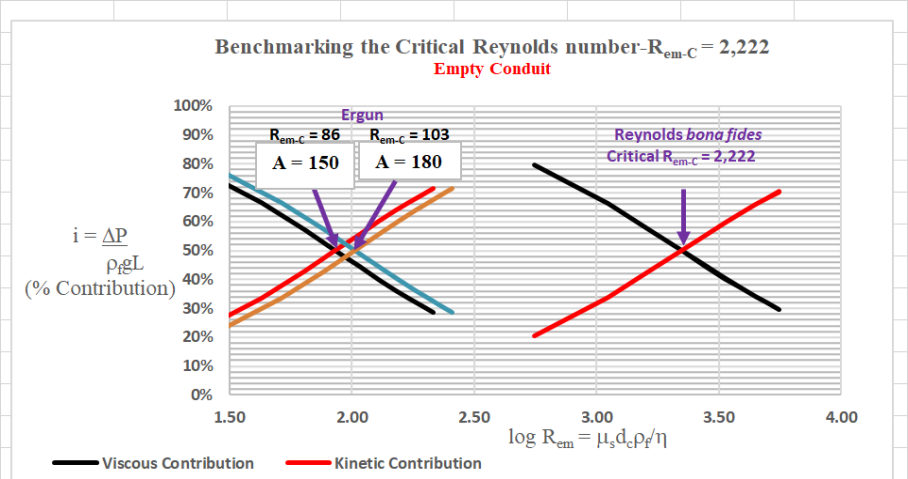

Fig. 7

Context for the Critical $R_{em\text{-}C}$ = 2222:

As has been pointed out in the QFFM original publication, Reynolds was not thorough in terms of strict fluid dynamics discipline when he settled on his definition of the now famous Reynolds number. Specifically, he ignored both the QFFM defined elements of porosity, δ, and wall-effect, λ. So, when his experiments yielded his critical value for $R_{em\text{-}C}$ = 2222, it lacks adjustment for both these two elements of fluid dynamics which were, nevertheless, present when he conducted his now famous experiment in the clear circular pipe with smooth walls. Fortunately, the additional fluid dynamic discipline is easily provided by the QFFM.

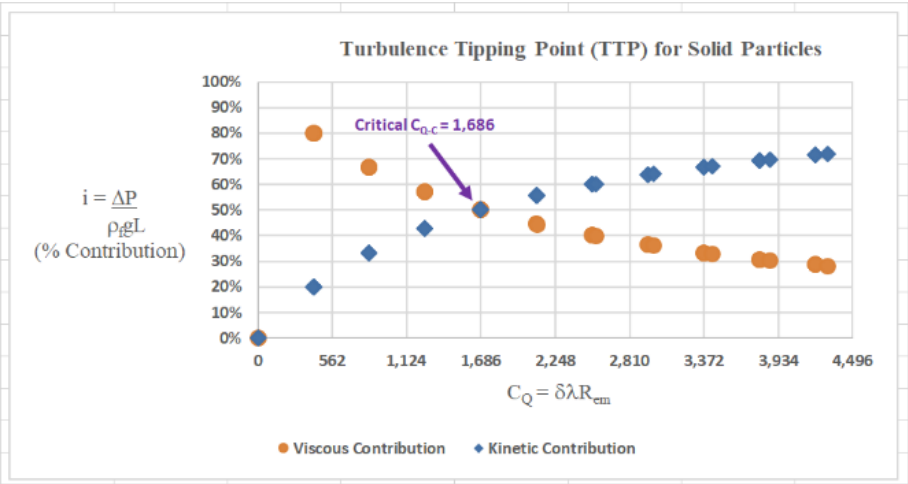

Fig. 8

As can be seen in Fig. 8, for a conduit packed with solid particles, the TTP is defined by the QFFM at the critical value of $C_{Q\text{-}C}$ =1686. Note that this critical value is normalized for both elements omitted by Reynolds, i.e., δ and λ.

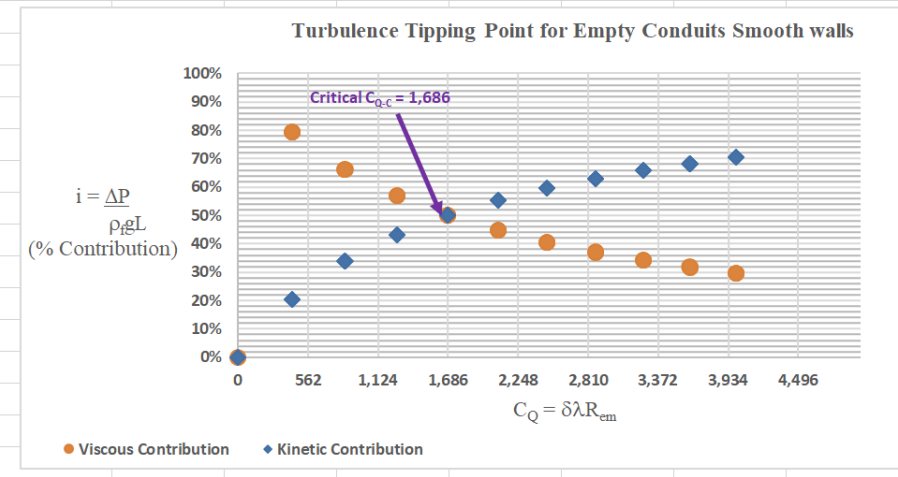

Fig. 9

Similarly, as can be seen in Fig. 9, for an empty conduit with smooth walls, the TTP is defined by the QFFM, also at the same critical value of $C_{Q\text{-}C}$ =1686. This is true because the QFFM normalized flow parameter, C_Q, is correctly normalized for all pertinent variables and, accordingly, the critical value for C_Q does not change for empty conduits or conduits packed with solid obstacles.

In order to connect the TTP value of $C_{Q\text{-}C}$ = 1686 and the critical Reynolds number value of $R_{em\text{-}C}$ = 2222, for an empty conduit, we need only use the conversion factor of $\delta\lambda$ = 6.07/8 = 0.7588, for an empty conduit with smooth walls. Thus, applying this conversion factor we get 2222 x 0.7588 = 1686.

QFFM Boundary Condition for TTP:

Applying our definition for the TTP in the QFFM, we can easily identify the boundary conditions for this extremely important benchmark in fluid dynamics. This is best accomplished as the relationship at TTP between dimensionless permeability Θ, and wall-effect parameter λ, as shown in the plot below.

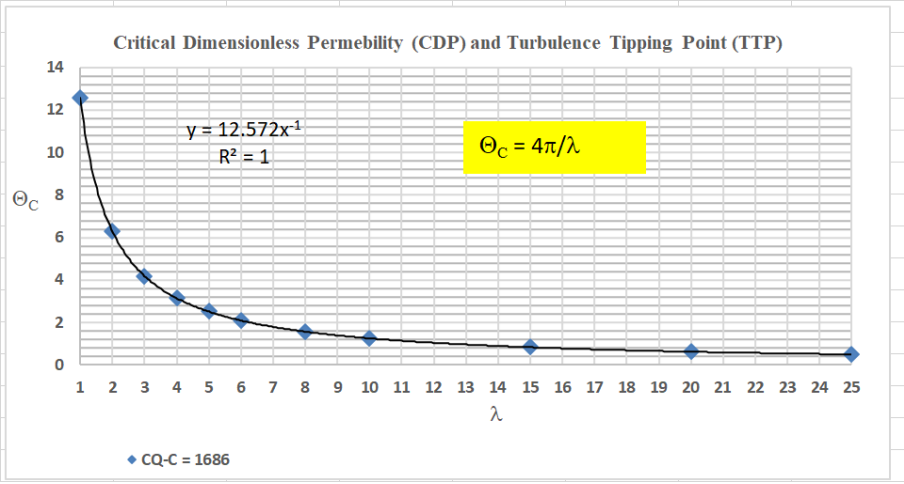

Fig. 10

As can be seen in Fig. 10, at the critical value of $C_{Q\text{-}C}$ = 1686, representing the TTP of fluid dynamics in closed conduits, dimensionless permeability is related to wall-effect as a reciprocal power function, i.e., $Q_C = 4\pi/\lambda$. Similarly, it can be shown that at the value $C_{Q\text{-}C}$ = 1686, the critical normalized pressure parameter $P_{Q\text{-}c} = 2k_1$. Thus, we can now add three new benchmarks to the portfolio of important fluid dynamic markers which define the TTP, i.e., $C_{Q\text{-}c}$ = 1.686, $Q_C = 4\pi/\lambda$ and $P_{Q\text{-}c} = 2k_1$ and, as validation, $k_1/k_2 = (64\pi/3)/(8\pi) = 512\pi^2/3 = 1{,}686$.

Reconciling Reynold's 1883 Experiments

In his original publication in 1883, Osborne Reynolds reported on experiments conducted in 5 different closed conduits which were empty tubes. Three of the conduits had smooth walls, Tube No.1, Tube No. 2 and Tube No. 3, and were made of glass which Reynolds used in combination with colored dyes to view, with the naked eye, the transition from Laminar to turbulent flow. Two of the conduits had roughened walls, Tube No.4 and Tube No. 5 and were made of lead and which he used to measure the relationship between fluid flow rate, q, and differential pressure through the conduits ΔP. We have captured the measured permeability data for these two latter conduits and compared the measured values to the QFFM calculated values to establish the correlation between the two. This correlation is shown below;

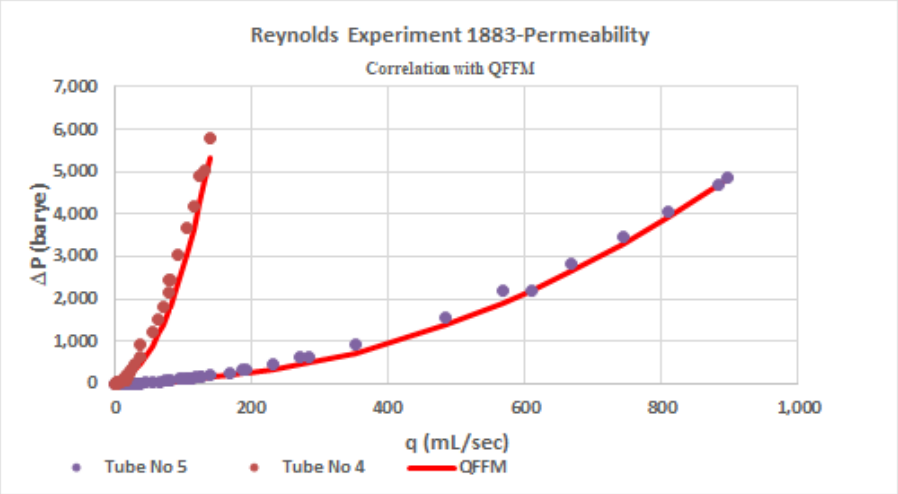

Fig. 11

As shown in Fig. 11, there is an excellent correlation between the measured and calculated values.

Next, we show the TTP for Reynold's experiments in Tube No 4 and Tube No. 5.

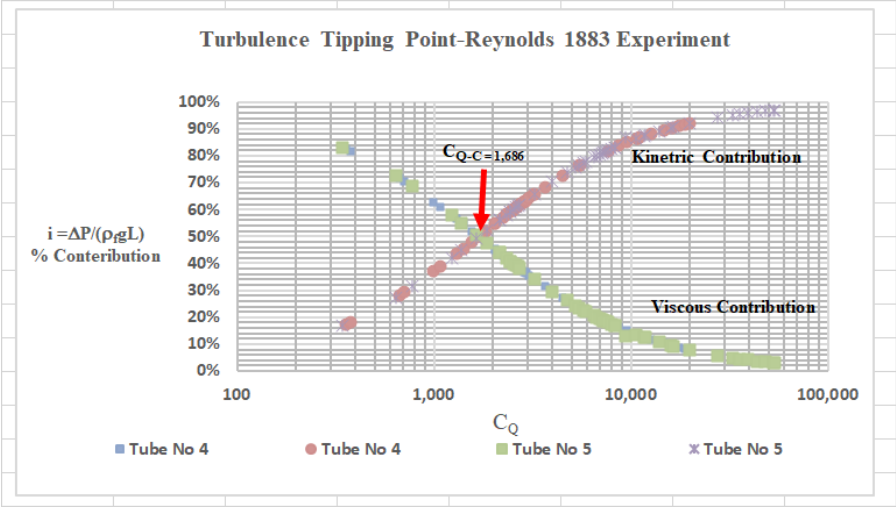

Fig. 12

As shown in Fig. 12, the TTP of Tube No. 4 and Tube No. 5 occurs at the critical value of C_Q = 1,686.

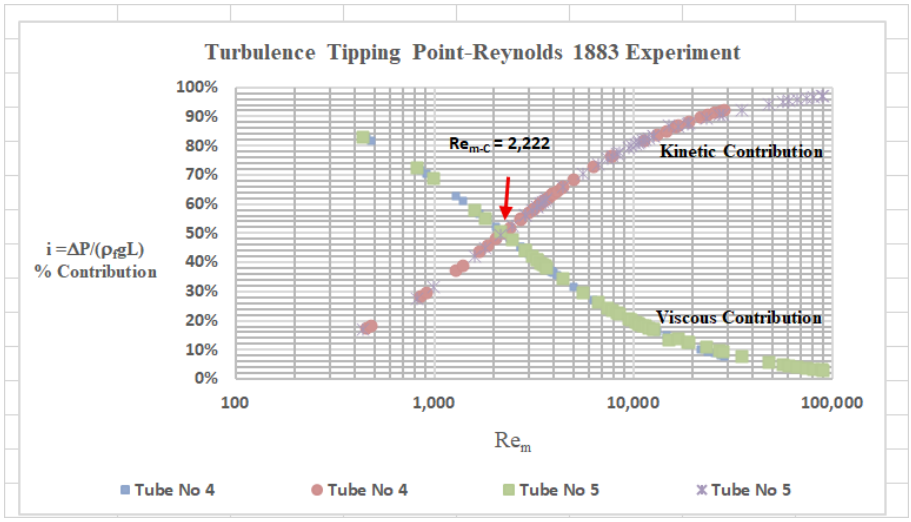

Fig. 13

Similarly, as shown in Fig. 13, the TTP occurs in Tube No. 4 and Tube N0. 5 at the critical value of Re_m = 2,222

Next, we evaluate tubes No. 4 and 5 in our dimensionless permeability plot shown below.

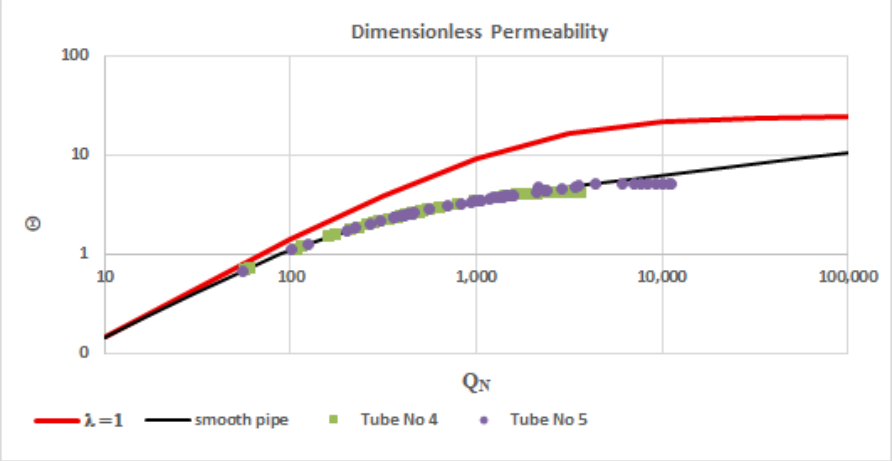

Fig. 14

As shown in Fig. 14, both tubes No. 4 and 5 show a slight deviation from that of a smooth surface at the higher values of Q_N. This small deviation is due to the roughness of the lead inner wall surface.

Finally, we show all results from the 5 Tubes in the Reynolds experiment in our universal frame of reference below.

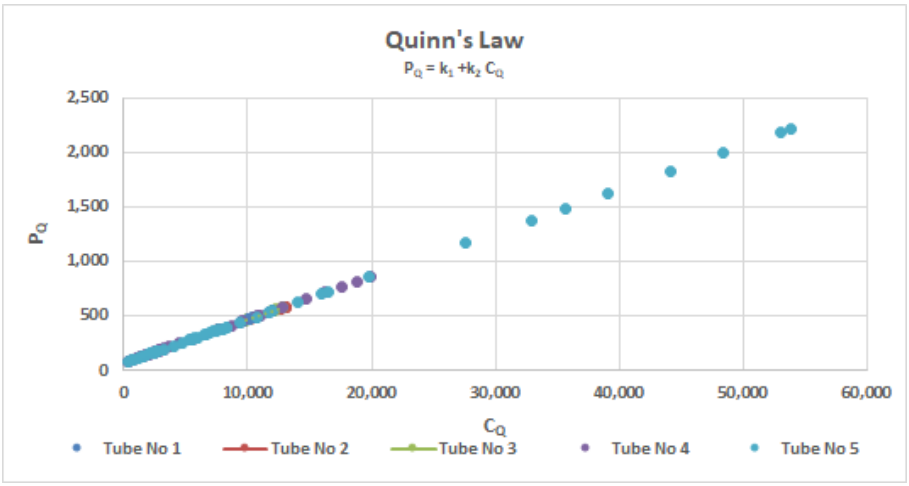

Fig. 15

As shown in Fig. 15, the results for all 5 tubes fall on the same straight line thus validating the robustness of the QFFM doctrine.

THE HARMONIC OSCILLATOR-TRANSITION TO TURBULENT FLOW EXPLAINED

We shall now develop the interrelationships among the conduit parameters which characterize the motion of the fluid within the HQC. Let Q be the position at any time t of a point describing a circle of radius a with uniform angular velocity ω about the center O. Let P be the projection of Q on any diameter A'OA. Let the angle AOQ = Φ. And let OP = x [See Figure 12].

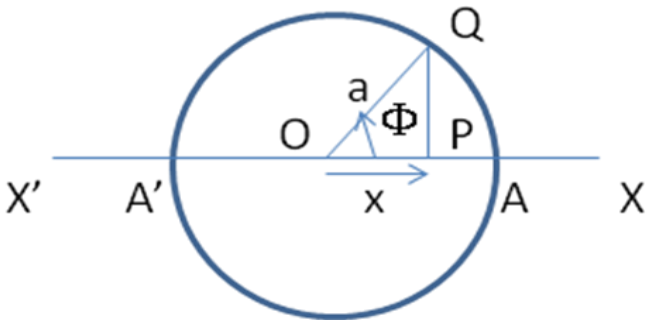

Fig. 16

Thus: d (Φ)/dt = ω, where ω is a constant. Hence; Φ = (ωt + α) where ω and α are constants Hence, x = a cos Φ = a cos (ωt + α).

We begin with the hypothesis that the motion of the fluid within the HQC is defined by that of uniform circular motion and, accordingly, the general equation of Simple Harmonic Motion (SHM), where, Φ = the phase of the motion; ω = the frequency of the motion; t = the elapsed time of the motion; α = the epoch of the motion, all as taught in the general theory of classical mechanics. Let us now apply this theoretical framework to the fluid motion within the HQC. Let $\Phi = P_Q$; $\omega = l/\phi_h$; $t = Q_N$; $\alpha = 2\pi k_1/360$; and $q = dV/dt$, where, P_Q = instantaneous HQC drag normalized viscous friction factor; ω = instantaneous HQC fluid resistance; λ = instantaneous HQC wall-adjusted fluid current normalization coefficient; ϕ_h = drag normalized hydraulic channel circumference; Q_N = instantaneous fluid current; k_1 = the drag normalized wetted surface area; and *V* = a control volume of fluid.

For clarity here, in our modeling of the fluid motion in the HQC, we recite our procedure of equating normalized *dimensionless* parameters related to the HQC to *dimensional* parameters in our SHM model. Thus, for instance, the dimensionless parameter Q_N of the HQC is equated to the elapsed time parameter t, of the SHM model, which has the dimensional units of seconds. Note also that we have *arbitrarily* chosen the units of *radians* in our definition of the epoch of the motion in the SHM model, by virtue of the unit conversion (2π/360), which is the conversion factor between degrees and radians. Thus, substituting for the terms which define our fluid motion in the HQC, we may now write, $P_Q = (k_1 + \lambda Q_N/\phi_h)$. It follows that we may state that, in the limit as Q_N tends to zero, the value of P_Q approaches the constant value of k_1. We can express this algebraical as; $P_Q = k_1$ in the limit as $Q_N \rightarrow 0$.

Thus, the function P_Q is bounded only on one side and varies from a minimum value of k_1 on the low side, when the fluid is at rest ($Q_N = 0$), and is unbounded on the high side (high value of Q_N). Let us define a corresponding HQC kinetic friction factor as: $P_K = P_Q/Q_N$, where, P_K = the instantaneous HQC normalized kinetic friction factor. Thus, the function P_K is *infinite* when the fluid is at rest ($Q_N = 0$). Driven by the principle of avoiding *non-finite* boundaries, let us define the reciprocal;$1/P_K = Q_N/P_Q = \Theta$, where, Θ = the dimensionless permeability of the HQC. It follows that we may write: $\Theta = 1/(k_1/Q_N + \lambda/\phi_h)$. It further follows that we may now state that, in the limit, as the value of Q_N tends to infinity: $\Theta = \phi_h/\lambda$. Similarly, we may state that, in the limit, as Q_N tends to zero: $\Theta = 0$.

Thus, the dimensionless permeability function of the HQC, Q, is *finite* on both sides and varies between the minimum limit of 0 on the low side and the maximum limit of ϕ_h/λ, on the high side.
The dimensionless parameters of the HQC are shown in Figure 17 below, in a log-log plot against Q_N.

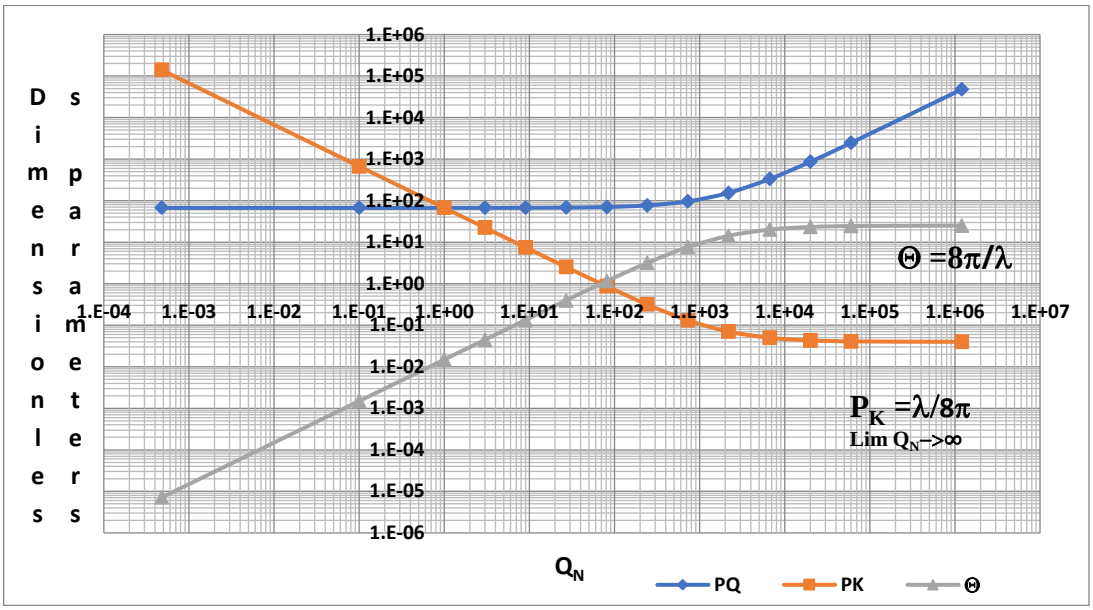

Fig. 17

As shown in Fig. 15, the fluid motion in the QHC is depicted in the form of dimensionless parameters over 11 orders of magnitude of the modified Reynolds number Re_m.

Modeling the HQC as a Harmonic Oscillator
The Spatial Coordinates:

We shall now return to the motion of the fluid within the HQC and describe it in terms of its instantaneous velocity coordinates in three dimensions, i.e., x, y, z. Thus, we may write: $v = v_x + v_y + v_z$, where, v = the total instantaneous velocity. Let us define the *conduit* frictional time interval as follows: $t_0 = \pi D^2 L \varepsilon_t/(4q)$, where, t_0 = time to displace one conduit volume of fluid. Let us define the *wall* shear stress as follows: $t_w = \Delta PD/(4L)$, where t_w = the wall shear stress. Let us define the frictional fluid velocity as follows: $\mu_f = \sqrt{(t_w/\rho_f)}$, where, μ_f = the frictional fluid velocity. Let us define the period of the fluid motion as follows: $T = 2\pi/\omega$, where, T = the period of the fluid motion. Let us define the frequency of the fluid motion as follows; $\phi = 1/T$, where, ϕ = the frequency of the fluid motion.

Let us define the maximum displacement amplitude of the fluid motion as follows: $M_0 = d_c/2$, where, M_0 = the maximum displacement amplitude of the fluid motion (scale factor). Let us define the instantaneous displacement amplitude as follows: $M = M_0 \exp^{(-\omega t0)}$, where, M = the instantaneous displacement amplitude of the fluid motion.

Note that the negative sign in the exponent represents the fact that the conduit wall frictional force acts in the opposite direction to the fluid motion and, hence, the motion is "damped" by wall friction. Let us define the instantaneous displacement amplitude in the x-axis plane as follows: $x = M\cos P_Q$, where, x = the instantaneous fluid displacement amplitude in the x-axis plane. Let us define the instantaneous fluid velocity in the x-axis plane as follows: $v_x = -M\lambda \sin P_Q/\phi_h$, where, v_x = the instantaneous fluid velocity in the x-axis plane. Let us define the instantaneous fluid acceleration in the x-axis plane as follows: $f_x = -M\lambda^2 \cos P_Q/\phi_h^2$, where, f_x = the instantaneous fluid acceleration in the x-axis plane. Let us define the instantaneous motion displacement in the y-axis plane as follows: $y = M\sin P_Q$, where, y = the instantaneous fluid displacement in the y-axis plane. Let us define instantaneous fluid velocity in the y-axis plane as follows: $v_y = M\lambda \cos P_Q/\phi_h$. where, v_y = the instantaneous fluid velocity in the y-axis plane. Let us define the instantaneous fluid acceleration in the y-axis plane as follows: $f_y = -M\lambda^2 \sin P_Q/\phi_h^2$, where, f_y = the instantaneous fluid acceleration in the y-axis plane. Let us define the instantaneous motion displacement in the z-axis plane as follows: $z = M\cos(\pi/4\text{-}P_Q)$, where, z = the instantaneous fluid displacement in the z-axis plane. Let us define the instantaneous fluid velocity in the z-axis plane as follows: $v_z = -M\lambda \sin(\pi/4\text{-}P_Q)/\phi_h$, where, v_z = the instantaneous fluid velocity in the z-axis plane. Let us define the instantaneous fluid acceleration in the z-axis plane as follows: $f_z = -M\lambda^2 \cos(\pi/4\text{-}P_Q)/\phi_h^2$, where, f_z = the instantaneous fluid acceleration in the z-axis plane.

The Hypothetical Q Unit Cell:

We shall now describe the dimensionless manifestation of the fluid motion in the HQC which we term the "Hypothetical Q Unit Cell" (HQUC). Let us define the *dimensionless* instantaneous motion displacement in the x-axis plane as follows: $x^* = x/M_0$, where, x^* = the dimensionless instantaneous fluid displacement in the x-axis plane.

Let us define the dimensionless instantaneous fluid velocity in the x-axis plane as follows: $v_x^* = v_x/\mu_f$, where, v_x^* = the dimensionless instantaneous fluid velocity in the x-axis plane. Let us define the dimensionless instantaneous motion displacement in the y-axis plane as follows: $y^* = y/M_0$, where, y^* = the dimensionless instantaneous fluid displacement in the y-axis plane. Let us define the dimensionless instantaneous fluid velocity in the y-axis plane as follows: $v_y^* = v_y/\mu_f$, where, v_y^* = the dimensionless instantaneous fluid velocity in the y-axis plane. Let us define the dimensionless instantaneous motion displacement in the z-axis plane as follows: $z^* = z/M_0$, where, z^* = the dimensionless instantaneous fluid displacement in the x-axis plane. Let us define the dimensionless instantaneous fluid velocity in the z-axis plane as follows: $v_z^* = v_z/\mu_f$, where, v_z^* = the dimensionless instantaneous fluid velocity in the z-axis plane.

The Fluid Current-Velocity Streamlines:

When the pressure gradient is unidirectional, as is the case in a walled conduit, the flow only occurs in the direction of the pressure gradient. We can show this by using Math Works ™ in MatLab™ software to plot the motion of the fluid as shown in Fig.18 below.

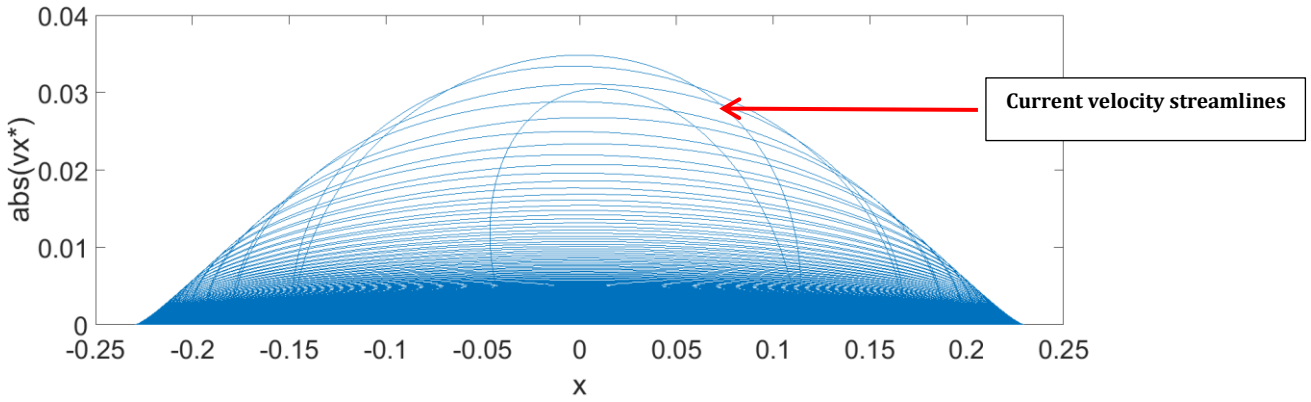

Fig. 18

As shown in Fig. 16, the scale of the motion is defined by the diameter of the HQC, i.e., d_c. In this example of an empty conduit, the diameter of the HQC is 0.46 cm and, accordingly, the maximum radius of the fluid flow profile is x = 0.23 cm. Note that the instantaneous speed is zero at both conduit walls (x = 0.23 cm, and x = -0.23 cm), i.e., the no slip boundary condition and reaches its maximum value in the center of the channel (x = 0 cm). The flow velocity profile goes from a *parabolic* type shape at low values of the fluid current Q_N (t) to almost flat at the highest values of Q_N (t). Accordingly, we refer to the velocity lines displayed as "current-velocity streamlines".

In the case where the pressure gradient is not uni-directional, we can view the fluid velocity profile in the x axis plane, as in Fig. 19 below.

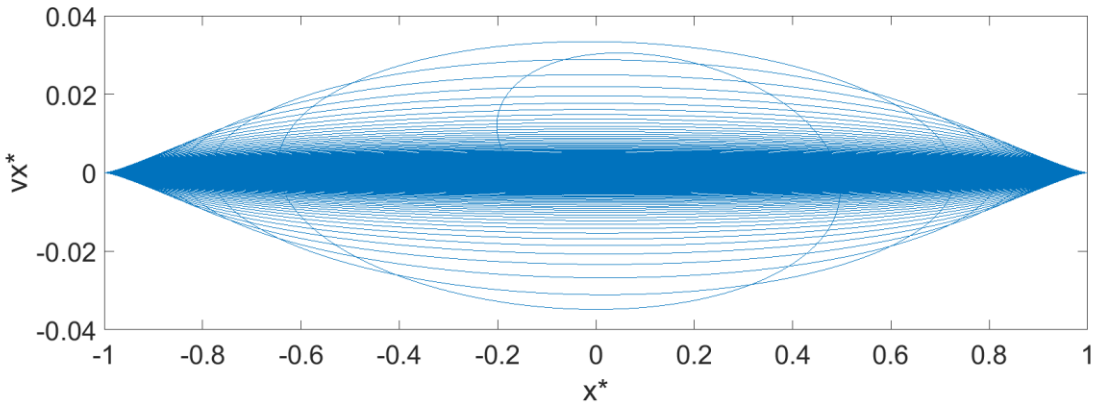

Fig. 19

As shown in Fig. 19, the instantaneous fluid speed is zero at the wall and maximum in the center of the channel. In addition, we can see the parabolic motion changing as a function of the value of the Q_N number. In this plot, the Q_N number increases towards the center from the top and bottom edges of the velocity streamlines.

Similarly, we can view the fluid velocity profile as a function of fluid current, Q_N, in the three-dimensional plane as shown in Fig. 20 below.

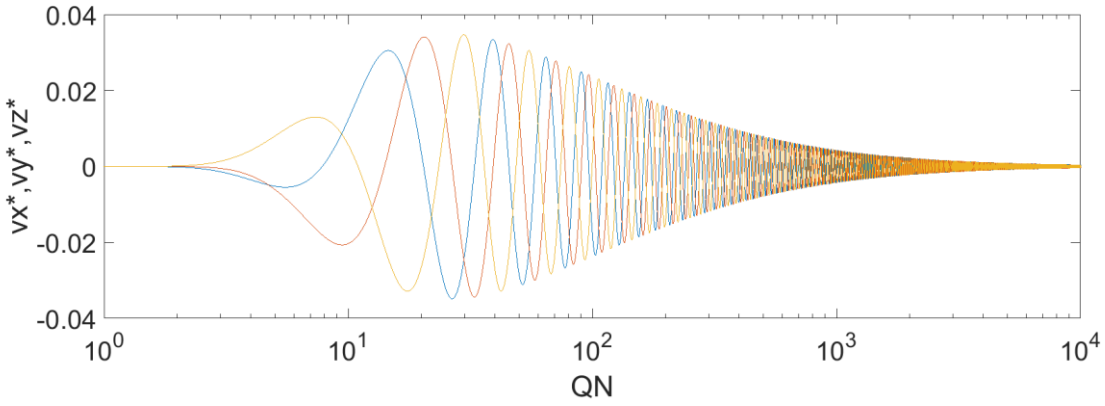

Fig. 20

As shown in Fig. 20, the changing fluid flow profile is captured as a function of fluid current using a log x axis. The damping effect of wall friction and fluid friction are apparent in this plot. Note that the amplitude of the wave initially increases due to the ever-decreasing wall friction. Having reached a maximum value when the wall fraction is minimized, it then decreases as the internal fluid friction becomes ever more dominant.

Similarly, the fluid motion in the HQC can be represented as a side view as shown in the Fig. 21 below.

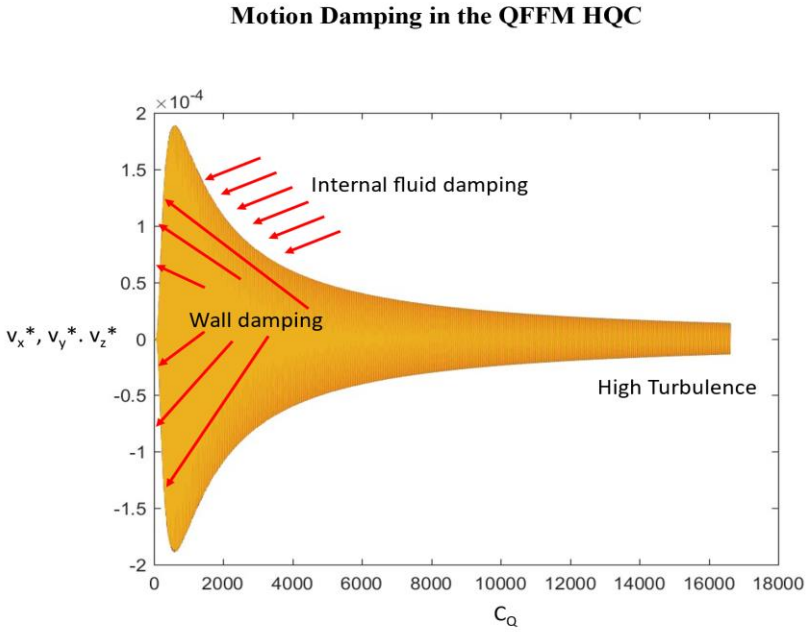

Fig. 21

As shown in Fig. 21, the two mechanisms of fluid motion damping can be seen. Wall friction damping manifest as the changing amplitude at relatively low values of C_Q, whereas the internal fluid damping manifests at higher values of C_Q.

ALL CONDUITS IN THE SAME FRAME OF REFERENCE-A COMPREHENSIVE VALIDATION

Finally, a major benefit of the QFFM is that we can view all the experimental data used in our validation protocol for both packed and empty conduits in the same frame of reference as a plot of Q versus Q_N, in Figure 22 below.

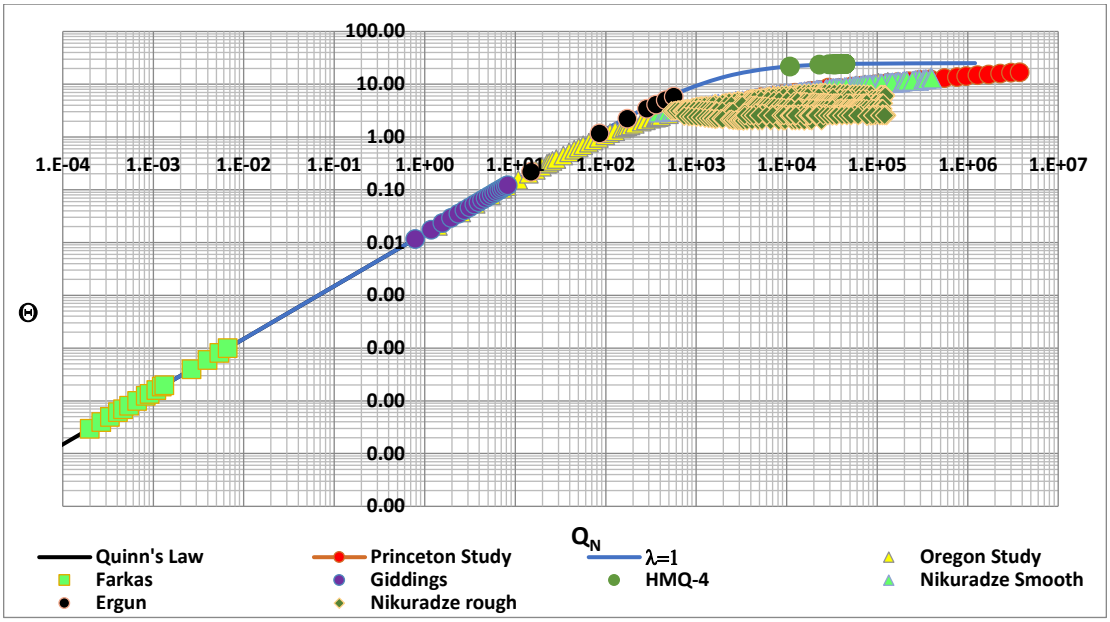

Fig. 22

As shown in Figure 22, this frame of reference differentiates between packed and empty conduits, on the one hand, and between smooth and roughened walls, on the other. Alternatively, we can view the entire validation data in the linear format of Quinn's Law, as a plot of P_Q versus C_Q, as shown in Figure 23 below.

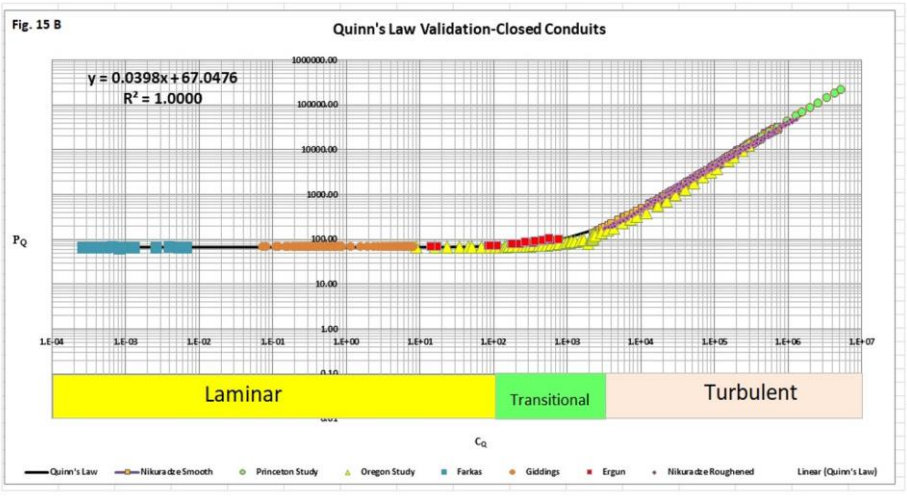

As shown in Fig, 23, our validation is shown over 13 orders of magnitude of the modified Reynolds number. This linear relationship between P_Q and C_Q is shown as a log/log plot to capture a landscape view of this unique depiction.

CONCLUSIONS

In this paper we have presented a comprehensive evaluation of the QFFM in light of the original experiments carried out by Osborne Reynolds in his classic paper of 1883. The following conclusions are drawn:

1. There is a compelling correlation between the permeability measurements taken by Reynolds in his 1883 experiments in lead tubes and the calculated values based upon the QFFM doctrine.
2. The conclusions reached by Reynolds concerning the onset of turbulent flow based upon his dye experiments in glass tubes are fully consistent with the damped simple harmonic motion outlined in the HQC doctrine of the QFFM.
3. The conclusion expressed by Reynolds in his original publication of 1883 concerning a value of 278 for the constant in laminar flow in the pressure/flow relationship in an empty conduit is in good agreement with the value of 270 taught by Giddings circa 1965 for a conduit packed with spherical particles.
4. The value of 278 taught by Reynolds is slightly higher than the value of 268 taught in the QFFM doctrine because Reynolds did not recognize the role of wall-effect, λ, which was present in his experiments carried out in the lead tubes.
5. The Turbulent Tipping Point (TTP) with a critical value for C_Q = 1,686, taught by the QFFM, is precisely validated by Reynold's experimental value for the critical value for Re_m = 2,222 in an empty conduit when adjusted for the QFFM parameters of δ and λ.
6. The Turbulent Tipping Point (TTP) is a more accurate bench-marker in fluid dynamics than the Kozeny constant because it represents the relative contributions of both viscous and kinetic contributions, not merely those of viscous origin.
7. Contrary to conventional wisdom, the QFFM teaches that turbulent flow is a highly structured flow, driven by the relative contributions of viscous and kinetic forces as the Reynolds number increases, rather than by random chaos.

References

[1] H. Darcy, Les Fontaines Publiques de la Ville de Dijon, Victor Dalmont, Paris, France, 1856

[2] H.S. de Azevedo, M.M. Franco, R.E.M. Morales, A.T. Franco, S.L.M. Junqueira, R.H.Erthal. Flow pattern and Friction Measurements of Turbulent Flow in Corrugated Pipes, *20th International Congress of Mechanical Engineering, November 15-20, 2009*.

[3] M.J. Baker, G.R. Tabor, Computational analysis of transitional air flow through packed columns of spheres using the finite volume technique. School of Engineering, Mathematics and Physical Sciences (SEMPS), Harrison Building, University of Exeter, North Park Road, Exeter, EX4 4QF, UK.

[4] E.Erdim, O. Algiray, I. Demir. A revisit of pressure drop-flow rate correlations for packed beds of spheres. Powder Technology 283 (2015) 488-504.

[5] N. Dukhan, O. Bagci, M. Ozdemir. Experimental flow in various porous media and reconciliation of Forchheimer and Ergun relations. Experimental Thermal and Fluid Science 57 (2014) 425-433.

[6] J.A. Anspach, T.D. Maloney, L.A. Colon. Ultrahigh-pressure liquid chromatography using a 1-mm id column packed with 1.5-mm porous particles. J. Sep. Sci. 2007, 30, 1207-1213.

[7] W. Zhong, K. Xu, X. Li, Y. Liao, G. Tao, T. Tagawa. Determination of pressure drop for air flow through sintered metal porous media using a modified Ergun equation. Advanced Powdered Technology xxx (2016) xxx-xxx.

[8] Tian et al/ J.Zhejiang, Pressure drop in a packed bed with sintered ore particles as applied to sinter coolers with a novel vertically arranged design for waste heat recovery. Applied Physics and Engineering 17 (2), 89-100, 2016.

[9] M. Mayerhofer, J. Govaerts, N. Parmentier, H. Jeanmart, L. Helsen. Experimental investigation of pressure drop in packed beds of irregular shaped wood particles. Powder Technology 205 (2011) 30-35.

[10] R. Pesic, T. K. Radoicic, N. Boskovic-Vragolovic, Z. Arsenijevic, Z. Grbavcici. Pressure drop in Packed beds of spherical particles at ambient and elevated temperatures. Chem. Ind. Chem. Eng. Q. 21 (3) 419-427 (2015).

[11] Z. T. Abidzaid, N. O. Kareem, M. N. Abbass. Modified Equations for Water Flow through Packed Bed for different types of packing systems. Iraqi Journal of Engineering Vol. 6 No 3, pp. 60-69

[12] Mirmanto. Developing Flow Pressure Drop and Friction Factor of Water in Copper Microchannels. Journal of Mechanics Engineering and Automation 3 (2013) 641-649.

[13] M.O.Carpinlioglu, E. Ozahi. A simplified correlation for fixed bed pressure drop. Powder Technology 187 (2008) 94-101.

[14] P. Yang, T. McCabe, M. Pursch. Practical comparison of LC columns packed with different superficially porous particles for the separation of small molecules and medium size natural products. J. Sep. Sci. 2011, 34, 2975-2982.

[15] S. Khayamyan, T.S. Lundstrom, J.U. G. Hellstrom, P. Gren, H. Lycksam. Measurement of Transitional and Turbulent Flow in a Randomly Packed Bed of Spheres with Particle Image Velocimetry. Transp. Porous Media (2017) 116: 413-431.

[16] E. Sletfjerding, J. Gudmundsson, K. Sjoeen. Flow Experiments with High Pressure Natural Gas In Coated And Plain Pipes. PSIG Annual Meeting, 28-30 October, 1998, Denver, Colorado

[17] L.I. Langeiandsvik, W. Postvolt, B. Aarhus, K.K. Kaste. Accurate Calculation of Pipeline Transport Capacity. Personal Communication, Gassco, AS.

[18] De Stephano et al, Characteristics of Superficially-Porous Silica Particles for Fast HPLC: Some Performance Comparisons with Sub-2-µm Particles. Journal of Chromatographic Science, Vol. 46, March 2008.

[19] L. Pereira, What Pressure to Expect from the Thermo Scientific Accucore HPLC Columns? Thermo Scientific Literature Technical Note 20542, 2012.

[20] J.H. Van Lopik, R. Snoeijers, T. C. G. W. Van Dooren, A. Raoof, R. J. Schotting. The Effect of Grain Size Distribution on Nonlinear Flow Behavior in Sandy Porous Media. Trahs Porous Media (2017) 120; 37-66.

[21] Z. Li, J. Wan, K. Huang, W. Chang, Y. He. Effects of particle diameter on flow characteristics in sand columns. International Journal of Heat and Mass Transfer 104 (2017) 533-536.

[22] Carman, P. C., "Fluid flow through granular beds", Transactions of the Institution of Chemical Engineers, vol. 15, pp. 155–166, 1937

[23] J. Kozeny, "Uber kapillare Leitung des wassers in Böden,"Sitzungsberichte der Kaiserlichen Akademie der Wissenschaften, vol. 136, pp. 271–306, 1927

[24] H. M. Quinn. Quinn's Law of Fluid Dynamics Pressure-driven Fluid Flow Through Closed Conduits. Fluid Mechanics. Vol. 5, No. 2, 2019, pp. 39-71. doi: 10.11648/j.fm.20190502.12

[35] F. E. Blake, "The resistance of packing to fluid flow,"Transaction of American Institute of Chemical Engineers, vol.14, pp. 415–421, 1922.

[25] M. Coulson; University of London, Ph. D. thesis, "The Streamline Flow of Liquids through beds comprised of Spherical particles" 1935

[26] G. Guiochon, S. G. Shirazi, A. M. Katti, Fundamentals of Preparative and Nonlinear Chromatography, Academic Press,Boston, Ma, (1994)

[27] H. M. Quinn, "Reconciliation of packed column permeability data, column permeability as a function of particle porosity, "Journal of Materials, vol. 2014, Article ID 636507, 22 pages, 2014.

[28] Quinn, H. M., A Reconciliation of Packed Column Permeability Data: Deconvoluting the Ergun Papers Hindawi Publishing Corporation Journal of Materials Volume 2014, Article ID 548482, 24 pages http://dx.doi.org/10.1155/2014/548482

[29] H.M. Quinn, Reconciliation of packed Column Permeability Data Part 1. The Teaching of Giddings revisited. Special Topics & Reviews in Porous media-An International Journal 1 (1). 79-86 (2010).

[30] S. Ergun and A. A. Orning, "Fluid flow through randomly packed columns and fluidized beds," Industrial & Engineering Chemistry, vol. 4, no. 6, pp. 1179–1184,1949.

[31] Ergun, Chem. Eng. Progr. 48 (1952) 89-94

[32] Bird, R. B., Stewart, W. E., Lightfoot, E. N. Transport Phenomena, John Wiley & Sons, Inc., p. 190.

[33] J.C. Giddings, Dynamics of Chromatography, Part I: Principles and Theory, Marcel Dekker, New York, NY, USA, 1965.

[34] J. C. Giddings, Unified Separation Science, John Wiley & Sons (1991).

[36] Forchheimer, P.: Wasserbewegung durch boden. Zeit. Ver. Deutsch. Ing 45, 1781–1788 (1901).

[37] T. Farkas, G. Zhong, G. Guiochon, Validity of Darcy's Law at Low Flow Rates in Liquid Chromatography Journal of Chromatography A, 849, (1999) 35-43

[38] A Thesis by C. Kang, PRESSURE DROP IN A PEBBLE BED REACTOR ,Submitted to the Office of Graduate Studies of Texas A&M University in partial fulfillment of the requirements for the degree of MASTER OF SCIENCE, August 2010.

[39] T. Buchwald, G. Schmandra, L. Schützenmeister, T. Fraszczak, T. Mütze, U. Peuker, Gaseous flow through coarse granular beds: The role of specific surface area Powder Technology 366 (2020) 821–831

[40] J. Nikuradze, NASA TT F-10, 359, Laws of Turbulent Flow in Smooth Pipes. Translated from "Gesetzmassigkeiten der turbulenten Stromung in glatten Rohren" VDI (Verein Deutsher Ingenieure)-Forschungsheft 356.

[41] J. Nikuradze, NACA TM 1292, Laws of Flow in Rough Pipes, July/August 1933. Translation of "Stromungsgesetze in rauhen Rohren." VDI-Forschungsheft 361. Beilage zu "Forschung auf dem Gebiete des Ingenieurwesens" Ausgabe B Band 4, July/August 1933.

[42] L. Prandtl, in Verhandlungen des dritten internationalen Mathematiker-Kongresses in Heidelberg 1904, A. Krazer, ed., Teubner, Leipzig, Germany (1905), p. 484. English trans. in Early Developments of Modern Aerodynamics, J. A. K. Ackroyd, B. P. Axcell, A. I. Ruban, eds., Butterworth-Heinemann, Oxford, UK (2001), p. 77.

[43] B.J. Mckeon, C.J. Swanson, M.V. Zagarola, R.J. Donnelly and A. J. Smits. Friction factors for smooth pipe flow; J.Fluid Mech. (2004), vol. 511, pp.41-44. Cambridge University Press; DO1;10.1017/S0022112004009796.

[44] B.J. Mckeon, M.V. Zagarola, and A. J. Smits. A new friction factor relationship for fully developed pipe flow; J.Fluid Mech. (2005), vol. 238, pp.429-443. Cambridge University Press; DO1;10.1017/S0022112005005501.

[45] C.J. Swanson, B. Julian, G. G. Ihas, and R. J. Donnelly. Pipe flow measurements over a wide range of Reynolds numbers using liquid helium and various gases. J. Fluid mech. (2002), vol. 461, pp.51-60. Cambridge University Press; DO1;10.1017/S0022112002008595.